Co-seismic Ionospheric disturbances induced by the Mw 7.4 Earthquake of April 2, 2024 in Hualien City, Taiwan

S. Bisht*(1), V. Chauhan#(1), R. Singh(2), A.R. Singh(1), V. Singh(3), and O.P. Singh(4)
(1) Department of Physics, Graphic Era Hill University, Dehradun-248002
(2) Department of Petroleum Engineering, Graphic Era (Deemed to be University), Dehradun-248002
(3)Department of Physics, St. John's College, Agra-282002
(4)Department of Applied Sciences & Humanities, Institute of Engineering & Technology, Lucknow-226021

Abstract

This study investigates the co-seismic ionospheric variations observed during the Taiwan earthquake (Mw 7.8) on April 2, 2024, using GPS data from two IGS stations: CKSV in Taiwan and PIMO in the Philippines. The total electron content (TEC) variations were analyzed, revealing significant anomalies following the earthquake. At CKSV, the VTEC values peaked at 24 TECU around 00:18 UTC before dropping sharply and stabilizing. In contrast, PIMO exhibited a steady increase in VTEC, reaching 37 TECU within an hour. The filtered VTEC data highlighted pronounced oscillations at CKSV with a peak of 0.51 TECU, while PIMO showed milder variations with smaller peaks. The anomalies were most significant for PRN-28, correlating with the propagation of earthquake-induced acoustic gravity waves (AGWs). These observations demonstrate the effectiveness of GPS-based TEC monitoring in detecting ionospheric disturbances caused by seismic activity. The results highlight the potential of TEC measurements as a valuable tool for earthquake precursory studies, providing crucial insights into the dynamic relationship between seismic events and ionospheric perturbations.

*Presenting author: snehabist28@gmail.com
#corresponding author: vishalchauhan@gehu.ac.in

1. Introduction

The study of earthquake processes and seismic anomalies is very important since seismic events are the most devastating natural phenomena that humans can encounter. The relationship between earthquakes and pre-earthquake ionospheric anomalies is a topic of interest in the field of seismology and ionospheric science. Researchers have observed that the earthquakes may induce changes in the ionosphere of the Earth during and before the significant events [1-10]. Many studies have focused on specific earthquakes, analyzing ionospheric data before and after the events [11]. In recent time, the use of GPS receivers has increased significantly for measuring the ionospheric total electron content (TEC) variations. The GPS system uses two frequencies for signal transmission, i.e. L1 and L2 at 1.5 GHz and 1.2 GHz respectively. This allows for ionospheric adjustment to be applied for accurate positioning readings. The GPS signals experience a delay between transmission and receiving time, caused by the ionospheric layers. This time delay can be used to estimate the TEC along the path between satellite and receiver on the ground [12].

Previous research has demonstrated that dense GPS arrays can be used as a most effective means to examine ionospheric perturbation. A study conducted from 1965 to 2013 on the seismo-ionospheric response of earthquakes revealed that only Mw > 6.5 earthquakes produce a significant wave response in the ionosphere [13]. According to Astafyeva et al. [14] shallow earthquakes with magnitude of about 7.8 produce significant co-seismic disturbances in the ionosphere. These disturbances are found to last about 4 to 8 minutes with a near-field amplitude of 0.2–0.4 TECU. Heki and Cahyadi's research explores the relationship between TEC and seismic activity. They discovered that anomalies in TEC often precede significant earthquakes. The study suggests that monitoring TEC could be a valuable tool in earthquake prediction, providing a potential early warning system for seismic events. Their findings highlight the interconnectedness of geophysical processes and underscore the importance of multidisciplinary approaches in earthquake forecasting [15].

In this paper, we are investigating the co-seismic ionospheric variations during the Taiwan earthquake (Mw7.8) of April 2, 2024.

2. Data and method of analysis

The Taiwan Mw7.4 earthquake occurred on 2nd April 2024 at 23:58:11 UTC, at a depth of 34.8 km with the epicenter occurring at 23.819ºN, 121.562ºE, located at 18 km SSW of Hualien city, Taiwan. For this study, we used the data from two IGS stations, i.e. CKSV, Taiwan and PIMO, Philippines. The coordinates of these stations are given in Table 1.

These two stations are considered because of their geographical location and availability of data. The TEC measurements are derived from the GPS data available at the IGS station in RINEX format. The method of analyzing TEC is explained by Marković et al.[16]. From RINEX format to VTEC calculation is done by using open software developed by Gopi Seemala (seemala.blogspot.in).

Table 1. Details of coordinates of IGS stations and their epicentral distance from the epicenter of April2, 2024 Taiwan earthquake (Mw7.8) and VTEC

S.No.	Station code	Lat. (°N)	Long. (°E)	Epicentral Distance (km)
1.	cksv	22.99	120.22	164
2.	pimo	14.63	121.07	1022

The VTEC values are mapped at sub-ionospheric height of 350 km, their mapping points are known as Iobnospheric Pierce Points (IPPs). These IPP locations can be used to see the path of different satellites at the subionospheric height. All the GPS satellites are assigned a unique PRN number. In this paper, significant variations are observed in the VTEC data of PRN-28 only. To identify the role of earthquake associated acoustic gravity waves (AGWs) in VTEC data; we applied a band pass filter of 01 to 10 mHz. The VTEC is measured in TECU and one TECU is equal to 1×10^{16} electrons per square meter.

3. Result and Discussion

By analyzing the VTEC data corresponding to the Mw7.8 Taiwan earthquake of April 2, 2024, it is found that only PRN-28 is showing significant variations. Since the time of occurrence of the earthquake is 23:58:11 UTC, the anomalous variations can be observed on the VTEC data of next day. Therefore, we plotted VTEC variations for April 3, 2024 in Figure 1. This figure shows two sets of graphs that compare the VTEC data for CKSV and PIMO stations over time. Every station consists of two graphs: one shows the VTEC data and the other filtered VTEC data.

It can be seen from Figure1(a) that at CKSV station the VTEC values ranges from 20 to 24 TECU at their peak around approximately 00:18 hours UT. Following their peak, the VTEC values drop for the next 10-12 minutes. At 00:30 hours UT the VTEC values return to about 21 TECU, where they remain stable for the rest of the period. At station PIMO (Figure 1b) there is a consistent increase in the VTEC values, which begin from approximately 30 TECU. During the one-hour duration, the VTEC attains approximately 37 TECU, exhibiting no notable decrease or variation. Figure 1(c), presenting the filtered VTEC data at CKSV station. It is peaking at approximately 0.51 TECU after 17 minutes at 00:15 hours (UTC). Figure 1(d) is showing variation of VTEC at PIMO station. At this station, the filtered VTEC data exhibits less noticeable variations than the CKSV. Throughout the measured period, the values fluctuate between -0.2 and 0.4 TECU with multiple small peaks, but without a prominent single peak as in CKSV. However, a smaller peak is seen about 30 minutes after the occurrence of the earthquake. This may be due to the larger epicentral distances from PRN-28. To see the epicentral distances from IPP locations of PRN-28 for both the stations we plotted them in Figure 2. According to the figure, the epicentral distance for PRN-28 grows with time for both the CKSV and PIMO data sets, with CKSV consistently recording shorter distances than PIMO It looks like the relationship is mostly linear, with a potential little curve suggesting an accelerated tendency. The epicentral distance has an increasing tendency over time, according to the CKSV and PIMO data sets. The epicentral distance for both stations grows over time. The epicentral distances from IPP location of PRN-28 from CKSV is always shorter than that recorded by PIMO for the course of the observed period, as evidenced by the fact that the CKSV data points are continuously lower than the PIMO data points. The plot's time range is 0 to 1 hour, indicating a steady and uninterrupted gathering of data points over this time.

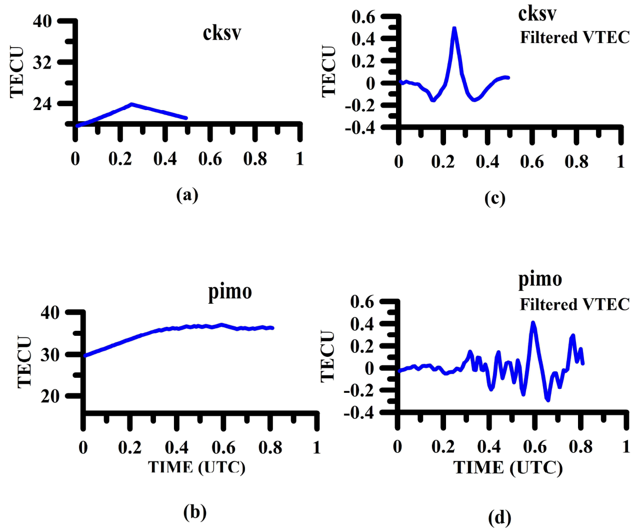

Figure 1.Variation of VTEC at CKSV station for the duration of one hour between 00:00 hrs and 01:00 hrs UT on April 03, 2024 (a), same as (a) but variation for PIMO station, Plot of band pass filtered VTEC at CKSV for the same duration of one hour on April 03, 2024 (c), same as (c) but variation for PIMO station.

CKSV indicates dynamic changes in the electron content, with a sharp rise and fall in the VTEC and notable oscillations in the filtered VTEC. PIMO shows a consistent rise in raw VTEC along with mild variations in filtered VTEC, indicating a more consistent and gradual change in electron content in contrast to CKSV. These observations demonstrate how the two stations' VTEC behaviors varied over time, with CKSV exhibiting more dynamic fluctuations and PIMO demonstrating a more steady and progressive increase.

The location of the epicenter, IGS stations and IPP locations of PRN-28 on April 3, 2024 are plotted in Figure 3. The map in the figure displays the locations of two stations, CKSV and PIMO as well as the blue lines represent IPP locations of PRN-28. The satellite track and the spatial distribution of these stations are shown visually on the map. The location of CKSV, indicated by a green triangle, is in northern Taiwan. The second green triangle indicates the location of PIMO, which lies in the Philippines, south of Luzon. The map shows two blue diagonal lines that cross the track of PRN 28. These lines show the satellite's route as it moves from the northeast to the southwest with respect to the surface of the Earth. In this figure, epicenter of the earthquake is shown by a red star. By illustrating how the satellite's path crosses the observation region that is serviced by the two stations, it draws attention to the spatial context in which the VTEC and epicentral distance data are being captured and evaluated.

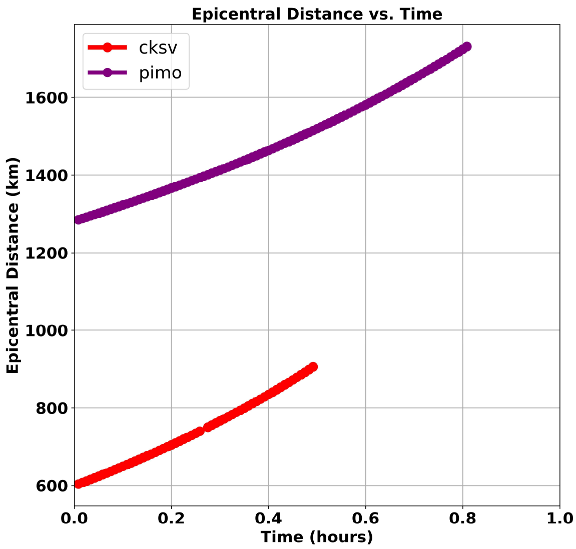

Figure 2.Plot of epicentral distances from each IPP locations of PRN-28 to the epicenter of Taiwan Mw7.8 earthquake of April 2, 2024.

Similar kinds of results have been observed by many other workers too but for other seismic events. For example, Chen et al.[17] reported seismic ionospheric disturbances (CIDs) within 10–13 minutes during the Lushan earthquake (M7.0) of April 20, 2013, Their analysis of GPS data revealed that the CIDs were small in amplitude and duration. These CIDs were found to be moved with a velocity consistent with sound wave propagation in the atmosphere. This suggests that CIDs originate from the acoustic waves produced by earthquakes. Further research is needed to examine the potential components for faster transmission during earthquake events. Cahyadi et al.[18] reported CIDs corresponding to the Palu earthquake (Mw 7.5) on September 28, 2018. 10-15 minutes after the earthquake, a TEC anomaly of 0.4 TECU was visible. After a checkerboard accuracy test, the 3D analysis showed CIDs north and south of the epicenter, with most of the positive anomalies occurring between 300 and 500 km above sea level, which is in line with the ionization properties of the F layer.

4. Conclusion

GPS data from CKSV and PIMO stations revealed strong co-seismic ionospheric disturbances (CIDs) following the Mw 7.4 earthquake that struck Hualien City, Taiwan, on April 2, 2024. The timing of these disruptions varied depending on how far away the stations were from the epicenter and were noticed within 17 minutes of the earthquake. These perturbation in VTEC were successfully identified by applying a band pass filter (1 mHz–10 mHz). This study demonstrating very well that the significant earthquakes can cause noticeable alterations in the ionosphere. The significance of GPS-based VTEC observations in tracking ionospheric reactions to seismic activity is highlighted by this work.

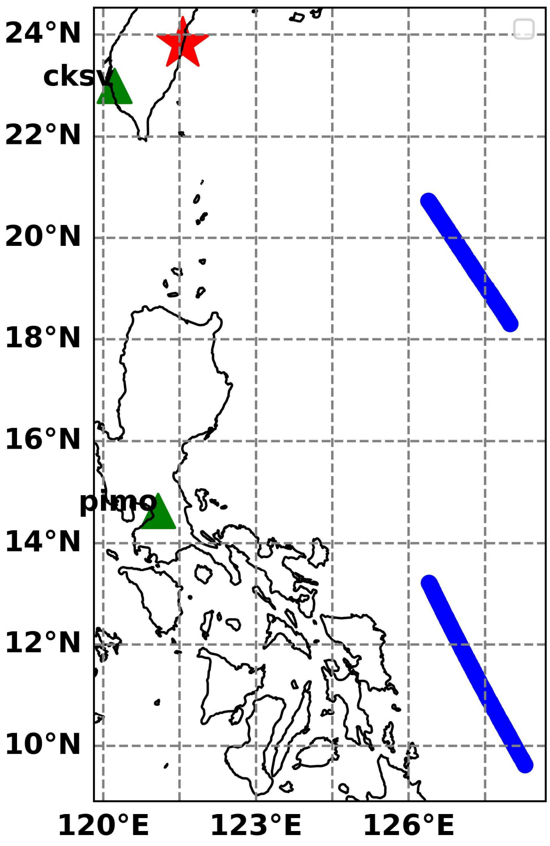

Figure 3.Plot of IPP locations of PRN-28 on April 3, 2024 between 00:00 hrs and 01:00 hrs UT. Here red star indicates the epicenter of the earthquake, green triangles denotes the location of IGS stations, and the blue line denotes the sub-ionospheric trajectory of PRN 28 for each station.

5. Acknowledgment

The authors express their gratitude to the Honorable Vice Chancellor of Graphic Era Hill University in Dehradun and

Graphic Era Deemed to be University in Dehradun for their support and for giving the necessary resources to conduct this research.

6. References

1. Le, H., Liu, J.Y., Liu, L., 2011. A statistical analysis of ionospheric anomalies before 736 M6.0+ earthquakes during 2002–2010. J. Geophys. Res. 116, A02303. http://dx.doi.org/10.1029/2010JA015781.

2. Le, H., Liu, L., Liu, J.Y., et al., 2013. The ionospheric anomalies prior to the M9.0 Tohoku-Oki earthquake. J. Asian Earth Sci. 62, 476–484. Liu, J.Y., Chen, Y.I., Pulinets, S.A., et al., 2000. Seimo-ionospheric signatures prior to MP6.0 Taiwan earthquakes. Geophys. Res. Lett. 27 (19), 3113–3116.

3. Liu, J.Y., Chen, Y.I., Pulinets, S.A., et al., 2000. Seimo-ionospheric signatures prior to MP6.0 Taiwan earthquakes. Geophys. Res. Lett. 27 (19), 3113–3116

4. Liu, J.Y., Chen, Y.I., Chuo, Y.J., et al., 2001. Variations of ionospheric total electron content during the Chi-Chi earthquake. Geophys. Res. Lett. 28 (7), 1383–1386.
5. Liu, J.Y., Chen, Y.I., Chuo, Y.J., et al., 2006. A statistical investigation of preearthquake ionospheric anomaly. J. Geophys. Res. 111, A05304.

6. Liu, J.Y., Chen, Y.I., Chen, C.H., et al., 2009. Seismoionospheric GPS total electron content anomalies observed before the 12 May 2008 Mw7.9 Wenchuan earthquake. J. Geophys. Res. 114, A04320.

7. Pulinets, S.A., Boyarchuk, K.A., 2004. Ionospheric Precursors of Earthquakes. Springer, New York, Berli

8. Yao, Y.B., Chen, P., Zhang, S., et al., 2012a. Analysis of pre-earthquake ionospheric anomalies before the global M = 7.0+ earthquakes in 2010. Nat. Hazards Earth Syst. Sci. 12 (3), 575–585.

9. Yao, Y.B., Chen, P., Wu, H., et al., 2012b. Analysis of ionospheric anomalies before the 2011 Mw9.0 Japan earthquake. Chin. Sci. Bull. 57 (5), 355–365.

10. Zhao, B., Wang, M., Yu, T., et al., 2008. Is an unusual large enhancement of ionospheric electron density linked with the 2008 great Wenchuan earthquake? J. Geophys. Res. 113, A11304.

11. Gautam, P. K., Chauhan, V., Sathyaseelan, R., Kumar, N., &Pappachen, J. P. (2018). Co-seismic ionospheric GPS-TEC disturbances from different source characteristic earthquakes in the Himalaya and the adjoining regions. *NRIAG Journal of Astronomy and Geophysics*, *7*(2), 237-246.

12. Trigunait, A., Parrot, M., Pulinets, S., Li, F., 2004. Variations of the ionospheric electron density during the Bhuj seismic event. Ann. Geophys. 22, 4123–4131.

13. Perevalova, N. P., Sankov, V. A., Astafyeva, E. I., &Zhupityaeva, A. S. (2014). Threshold magnitude for ionospheric TEC response to earthquakes. *Journal of Atmospheric and Solar-Terrestrial Physics*, *108*, 77-90.

14. Astafyeva, E., Lognonné, P., Rolland, L., 2011. First ionosphere images for the seismic slip of the Tohoku-oki earthquake. Geophys. Res. Lett. 38, L22104.

15. Cahyadi, M.N., Heki, K., 2015. Coseismic ionospheric disturbance of the large strike-slip earthquakes in North Sumatra in 2012: Mw dependence of the disturbance amplitudes. Geophys. J. Int. 200, 116–129.
16. Marković, M. (2014). Determination of total electron content in the ionosphere using GPS technology. *Geonauka*, *2*(4), 1-9.

17. Chen, P., Yao, Y., Chen, J., Yao, W., & Zhu, X. (2014). Study of the 2013 Lushan M7. 0 earthquake coseismic ionospheric disturbances. *Advances in Space Research*, *54*(11), 2194-2199.

18. Cahyadi, M. N., Arisa, D., Muafiry, I. N., Muslim, B., Rahayu, R. W., Putra, M. E., & Wulansari, M. (2022). Three-Dimensional Tomography of Coseismic Ionospheric Disturbances Following the 2018 Palu Earthquake and Tsunami from GNSS Measurements. *Frontiers in Astronomy and Space Sciences*, *9*, 890603.